

Electronic Supplementary Information

Photothermal Möbius Aromatic Metallapentalenofuran and Its NIR-Responsive Copolymer

Zhengyu Lu,^{a,b} Yuanting Cai,^b Yuanqing Wei,^b Qin Lin,^a Jiangxi Chen,^{*,a} Xumin He,^b Shunhua Li,^b Weitai Wu^b and Haiping Xia^{*,b}

^aDepartment of Materials Science and Engineering, College of Materials, Xiamen University, Xiamen 361005, People's Republic of China.

^bState Key Laboratory of Physical Chemistry of Solid Surfaces and Collaborative Innovation Center of Chemistry for Energy Materials (iChEM), College of Chemistry and Chemical Engineering, Xiamen University, Xiamen 361005, People's Republic of China.

Contents

1. Spectroscopic Data	S2
2. X-ray molecular structure for 9	S15

1. Spectroscopic Data

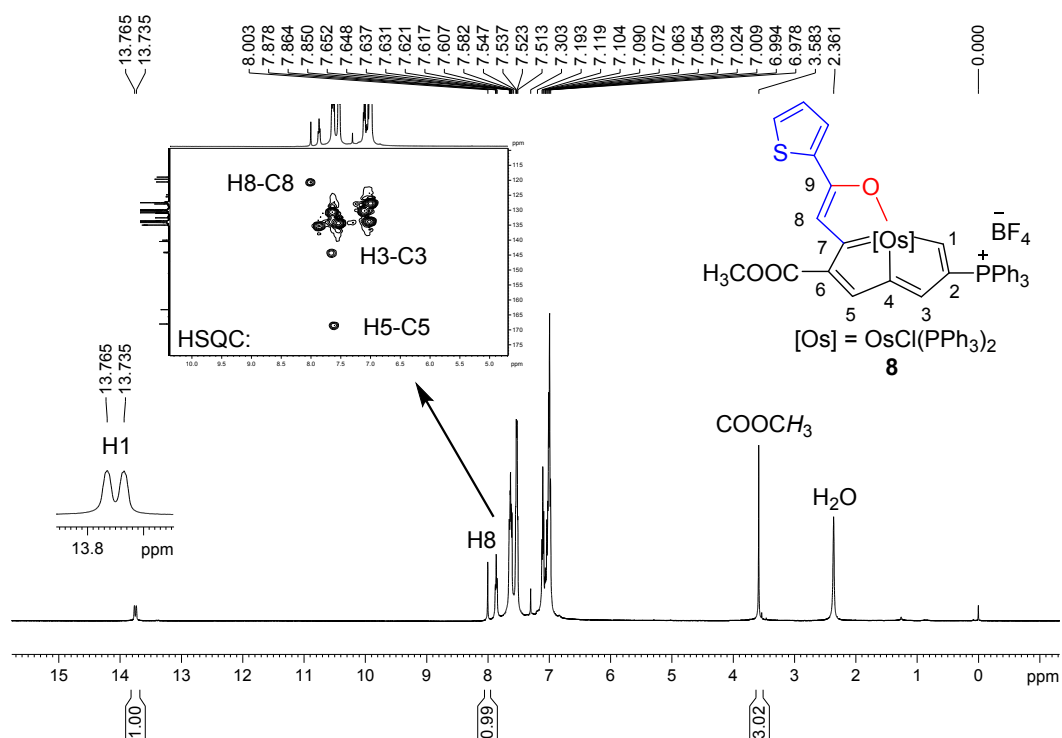


Figure S1 The ^1H NMR (500.2 MHz, CDCl_3) spectrum (inset: partial ^1H - ^{13}C HSQC spectrum) for complex **8**.

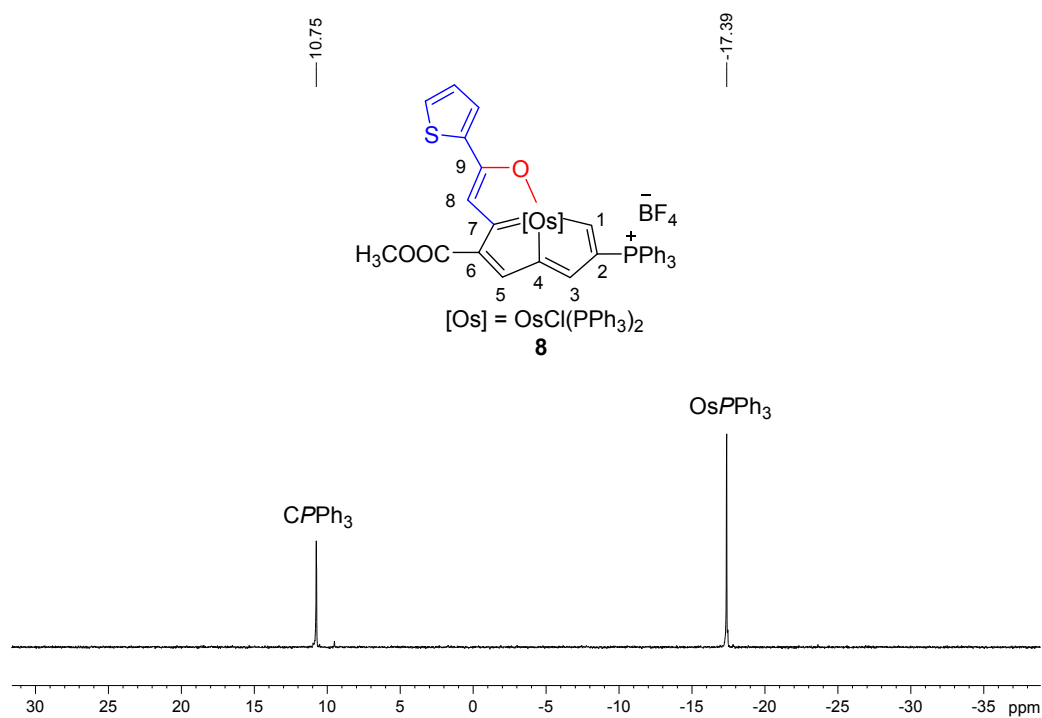


Figure S2 The $^{31}\text{P}\{^1\text{H}\}$ NMR (202.5 MHz, CDCl_3) spectrum for complex **8**.

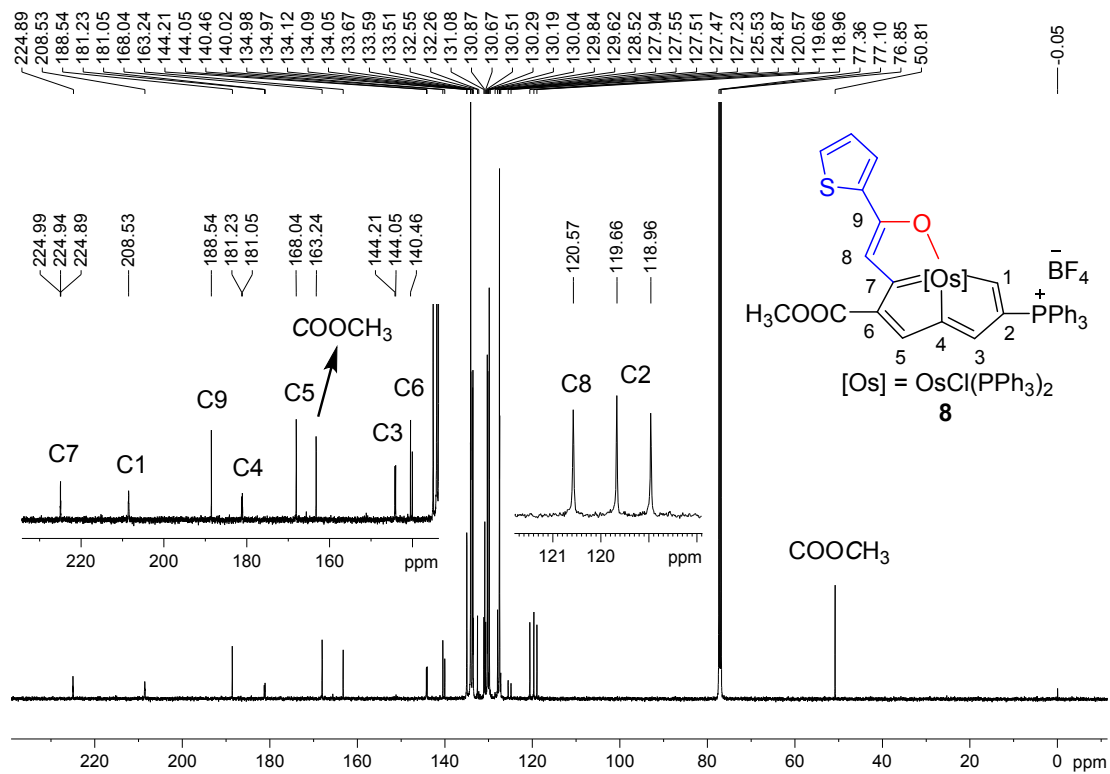


Figure S3 The $^{13}\text{C}\{^1\text{H}\}$ NMR (125.8 MHz, CDCl_3) spectrum for complex **8**.

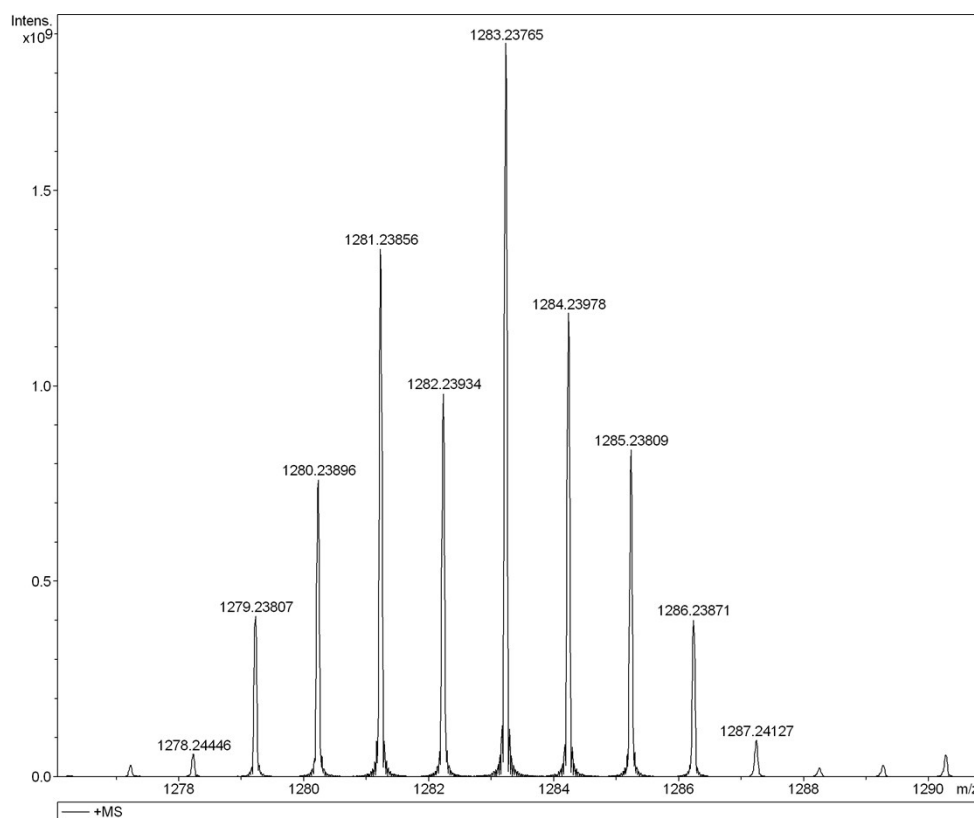


Figure S4. Positive-ion ESI-MS spectrum of $[\mathbf{8}]^+$ measured in dichloromethane.

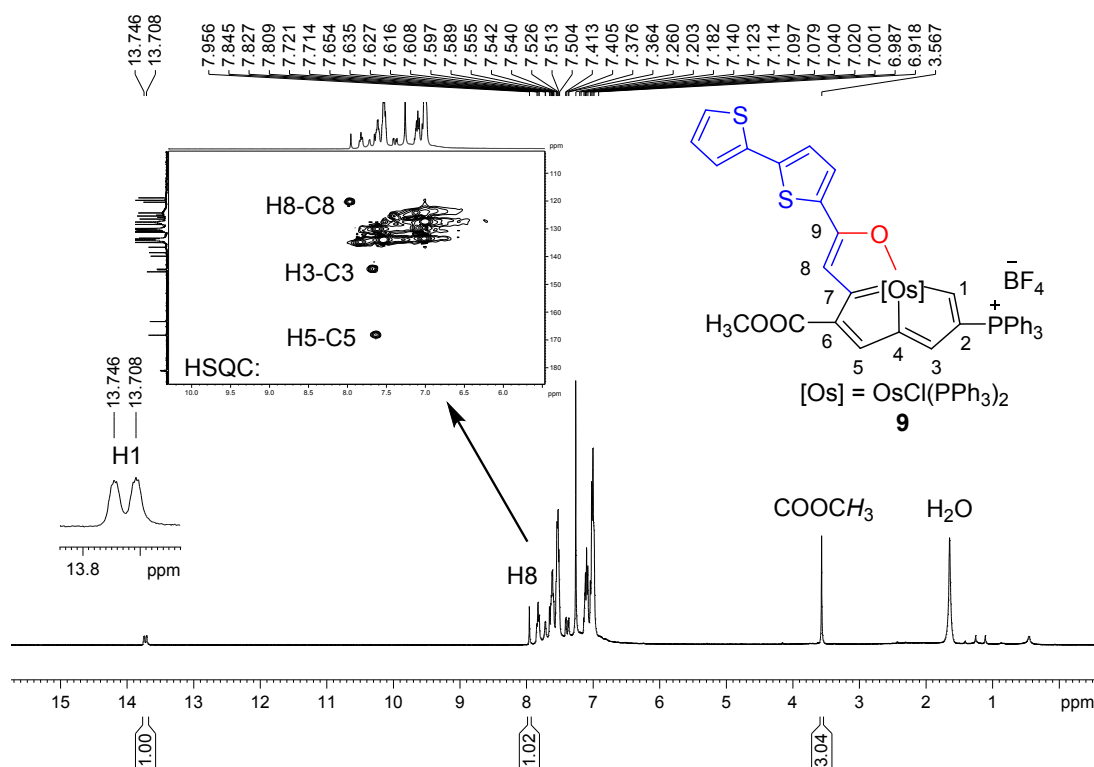


Figure S5 The ^1H NMR (400.1 MHz, CDCl_3) spectrum (inset: partial ^1H - ^{13}C HSQC spectrum) for complex **9**.

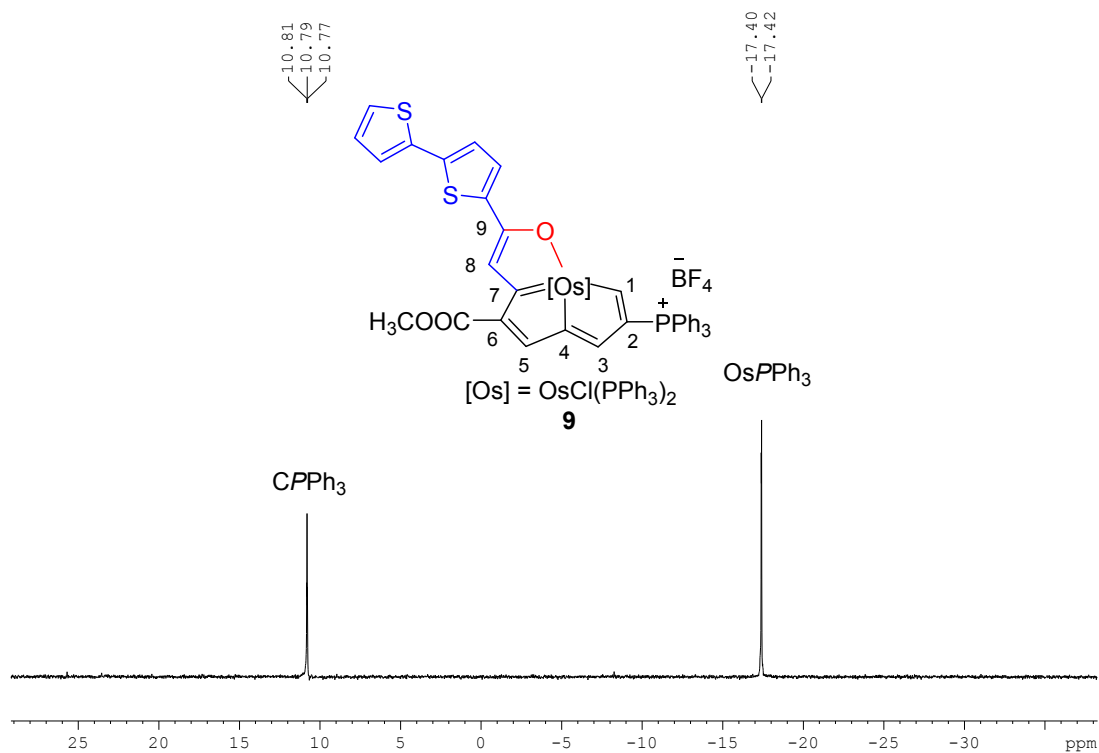


Figure S6 The $^{31}\text{P}\{^1\text{H}\}$ NMR (162.0 MHz, CDCl_3) spectrum for complex **9**.

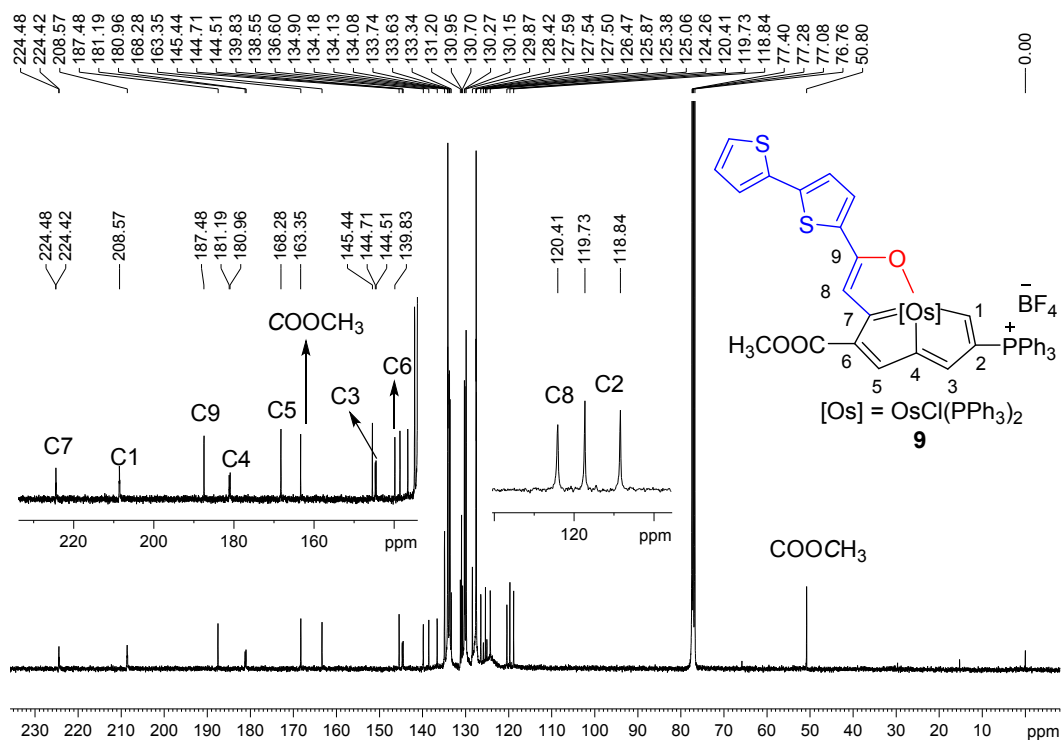


Figure S7 The $^{13}\text{C}\{^1\text{H}\}$ NMR (100.6 MHz, CDCl_3) spectrum for complex **9**.

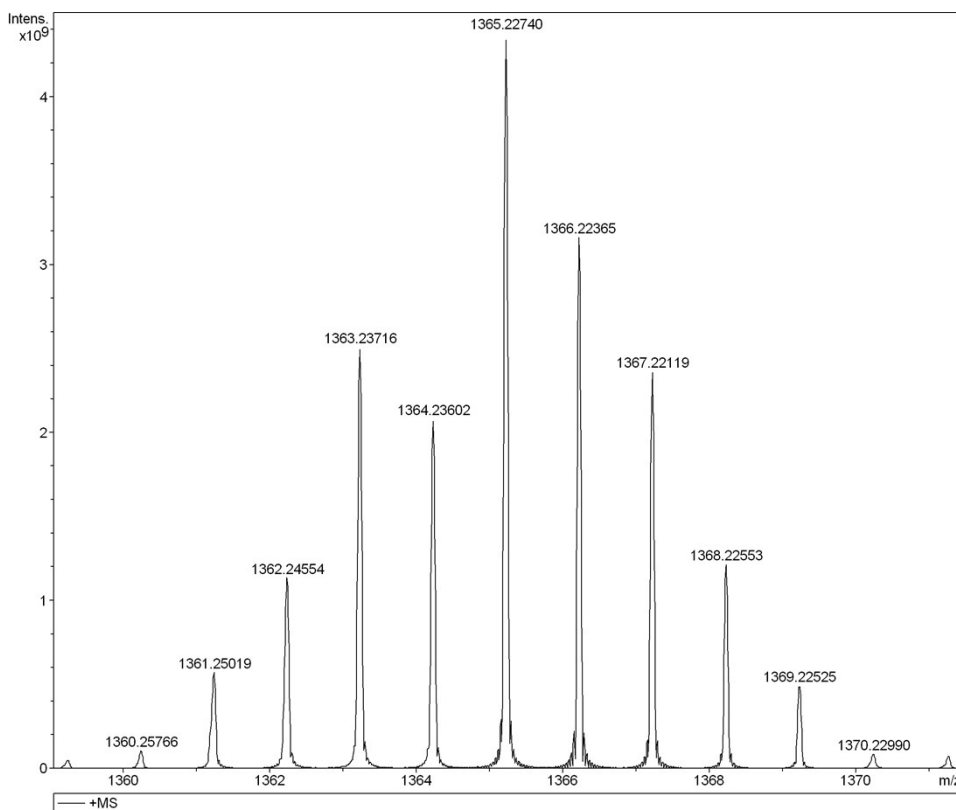


Figure S8 Positive-ion ESI-MS spectrum of $[\mathbf{9}]^+$ measured in dichloromethane.

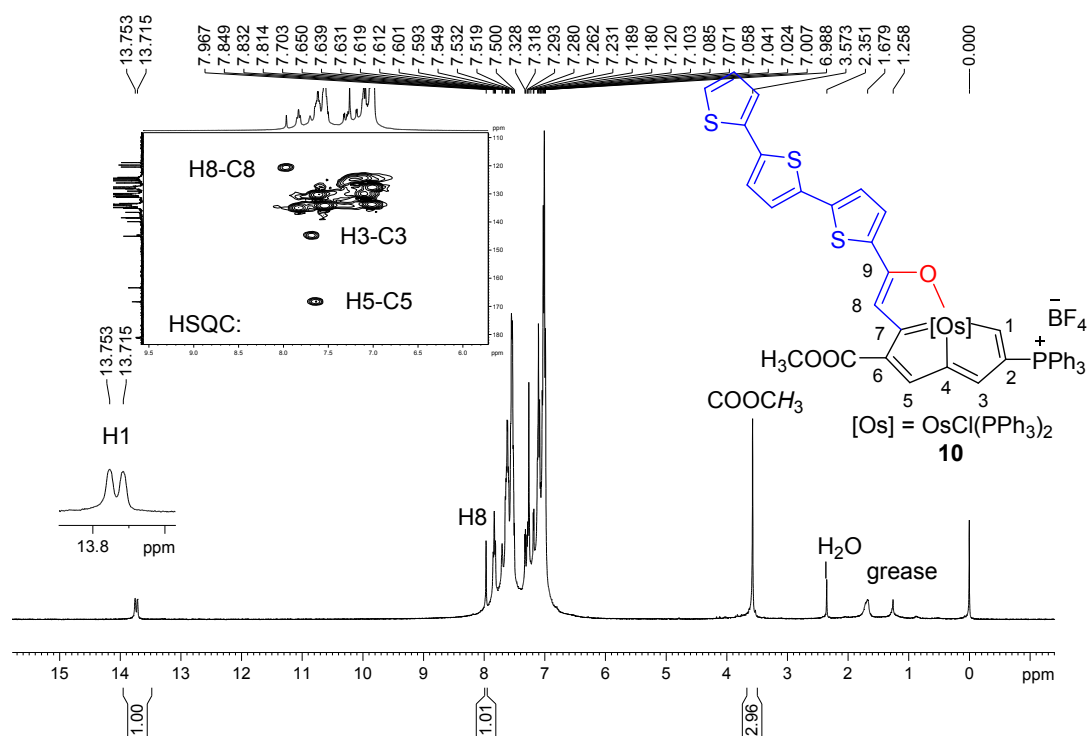


Figure S9 The ^1H NMR (400.1 MHz, CDCl_3) spectrum (inset: partial ^1H - ^{13}C HSQC spectrum) for complex **10**.

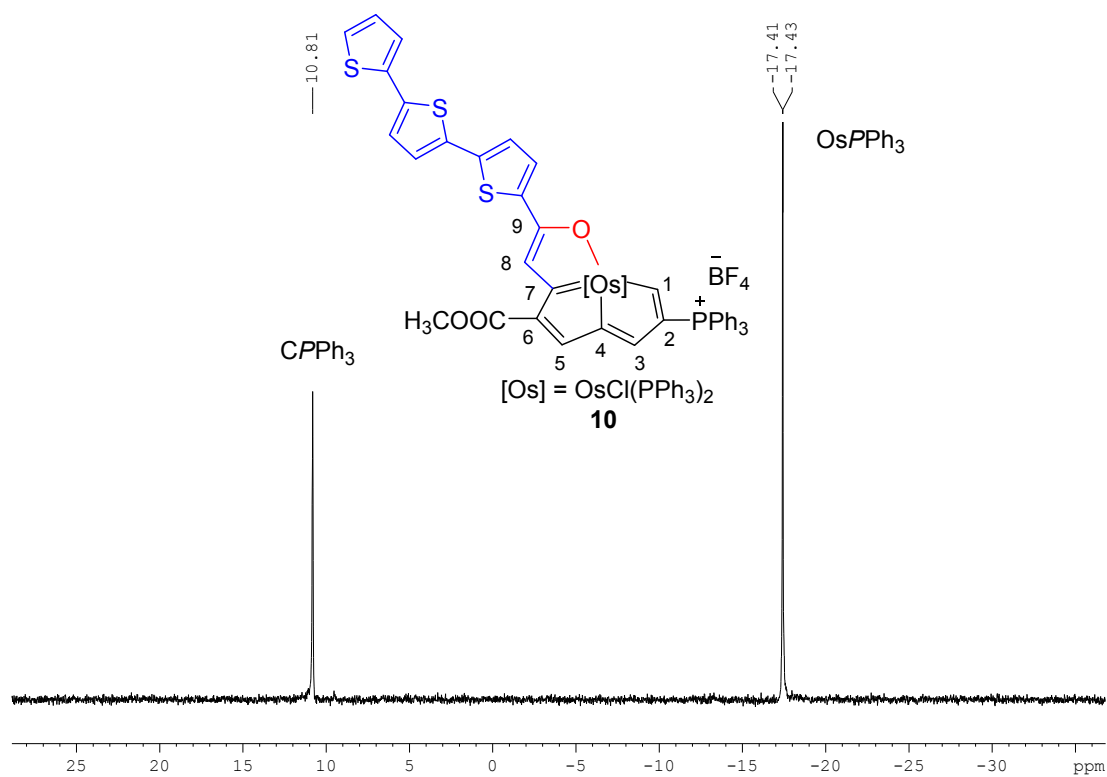


Figure S10 The $^{31}\text{P}\{^1\text{H}\}$ NMR (162.0 MHz, CDCl_3) spectrum for complex **10**.

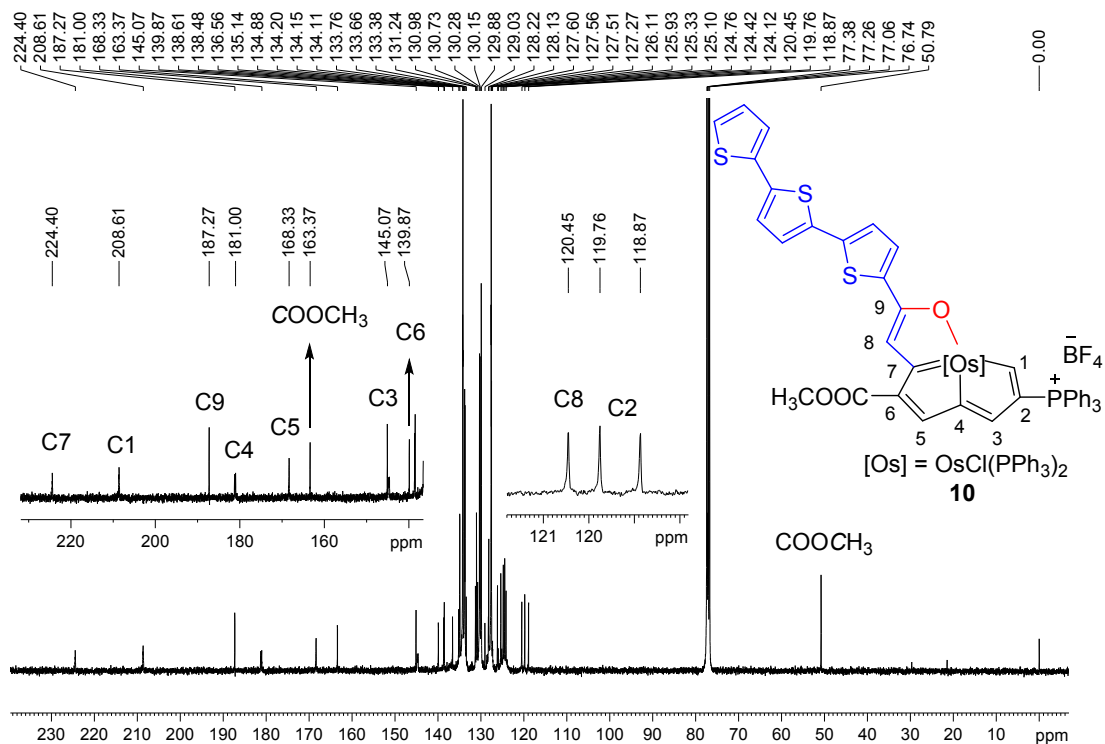


Figure S11 The $^{13}\text{C}\{^1\text{H}\}$ NMR (100.6 MHz, CDCl_3) spectrum for complex **10**.

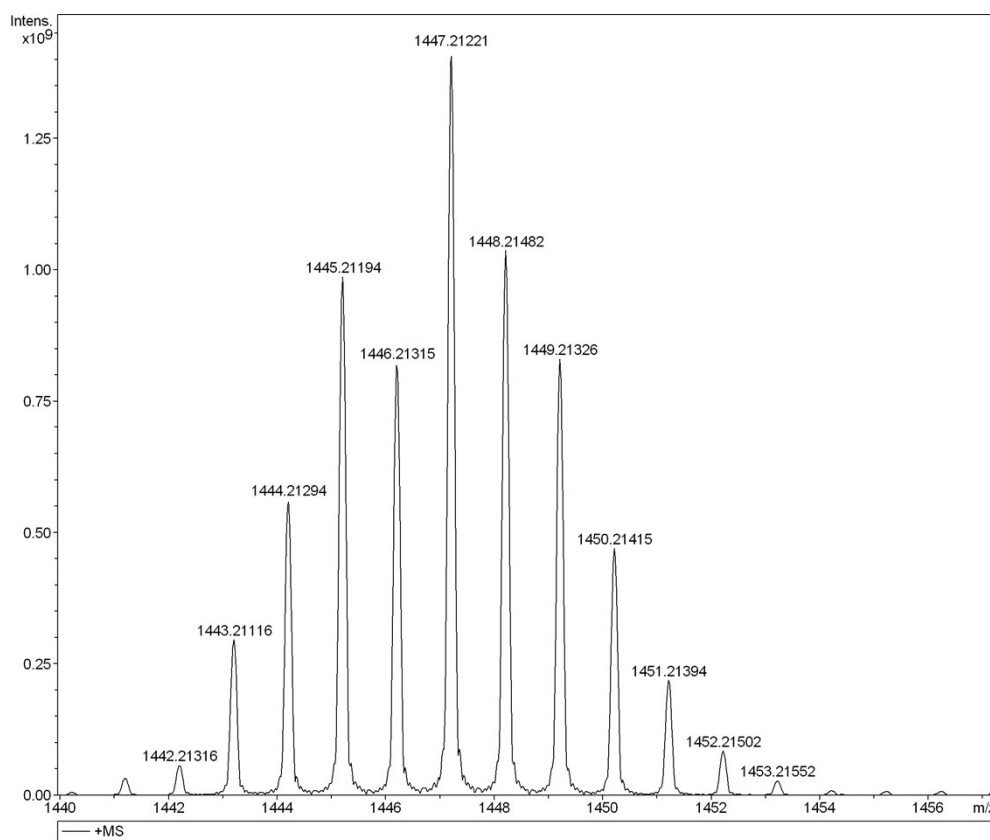


Figure S12 Positive-ion ESI-MS spectrum of $[\mathbf{10}]^+$ measured in dichloromethane.

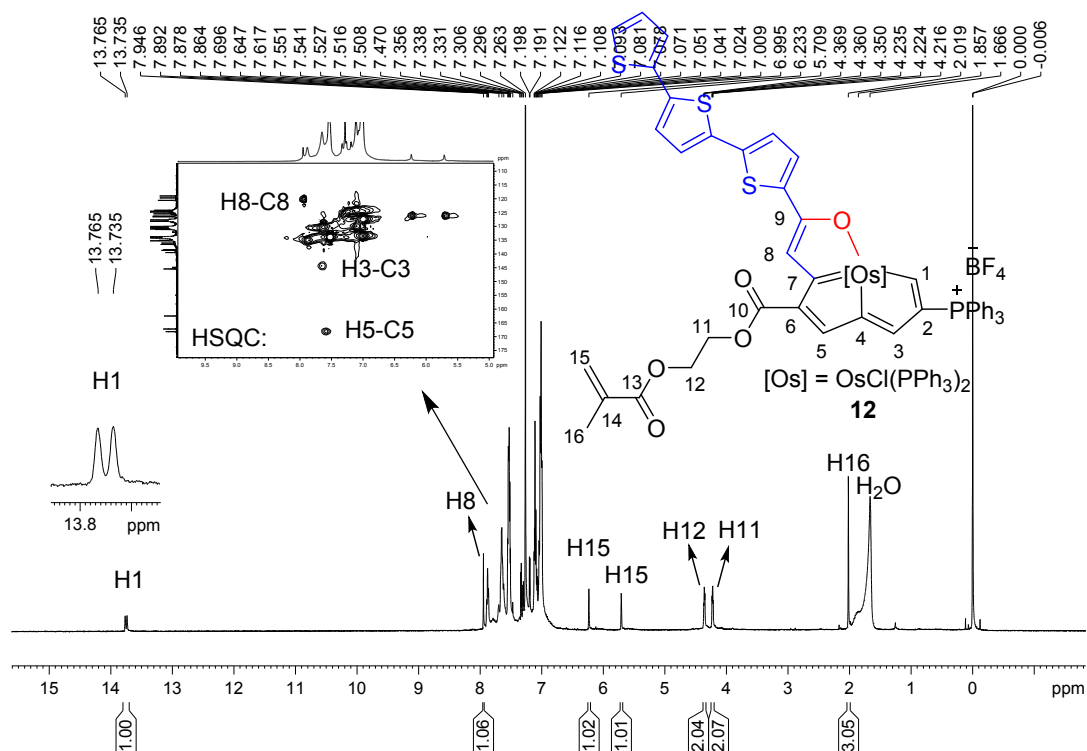


Figure S13 The ^1H NMR (500.2 MHz, CDCl_3) spectrum (inset: partial ^1H - ^{13}C HSQC spectrum) for complex **12**

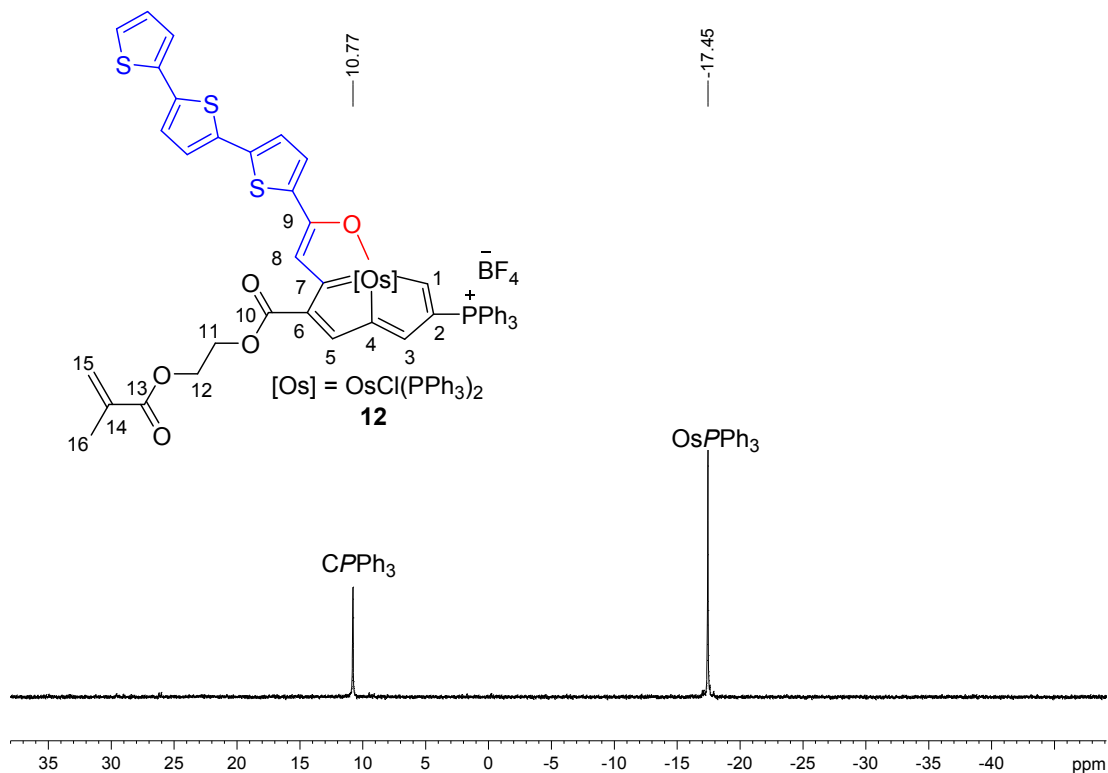


Figure S14 The $^{31}\text{P}\{^1\text{H}\}$ NMR (202.5 MHz, CDCl_3) spectrum for complex **12**

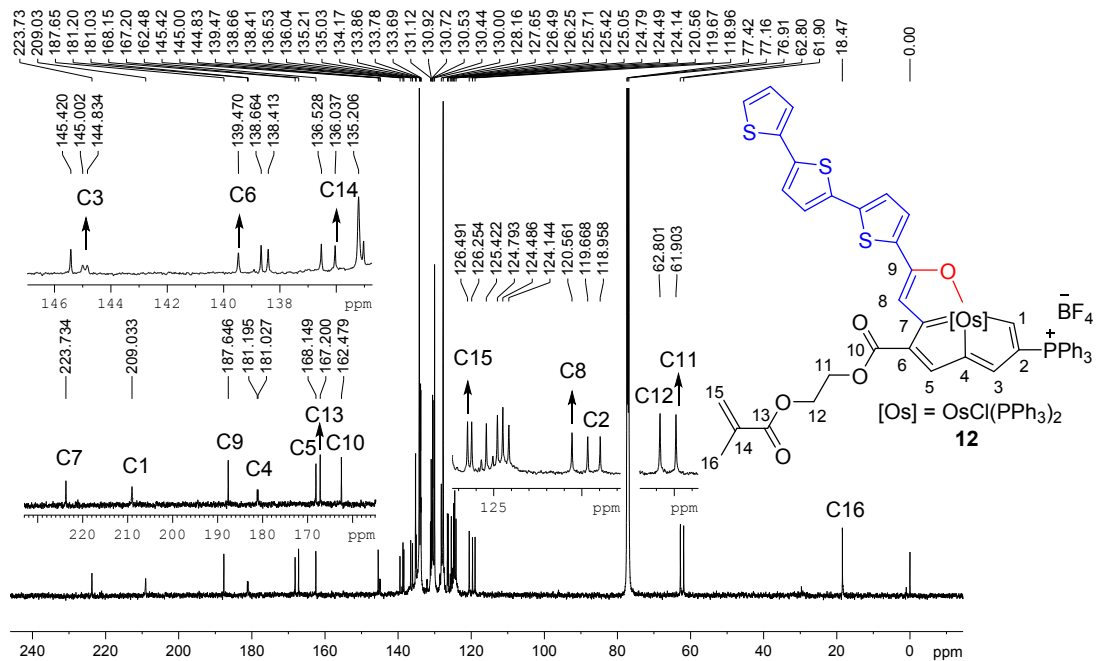


Figure S15 The $^{13}\text{C}\{^1\text{H}\}$ NMR (125.8 MHz, CDCl_3) spectrum for complex **12**

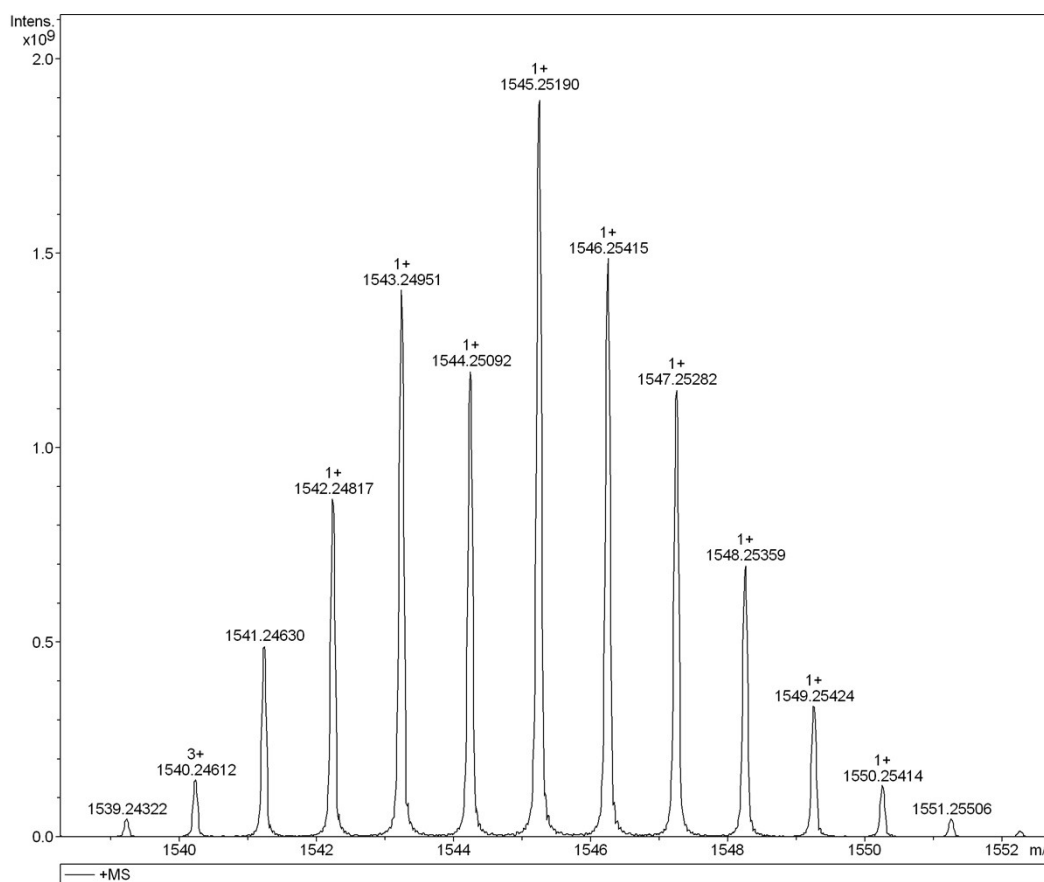


Figure S16 Positive-ion ESI-MS spectrum of $[\mathbf{12}]^+$ measured in dichloromethane.

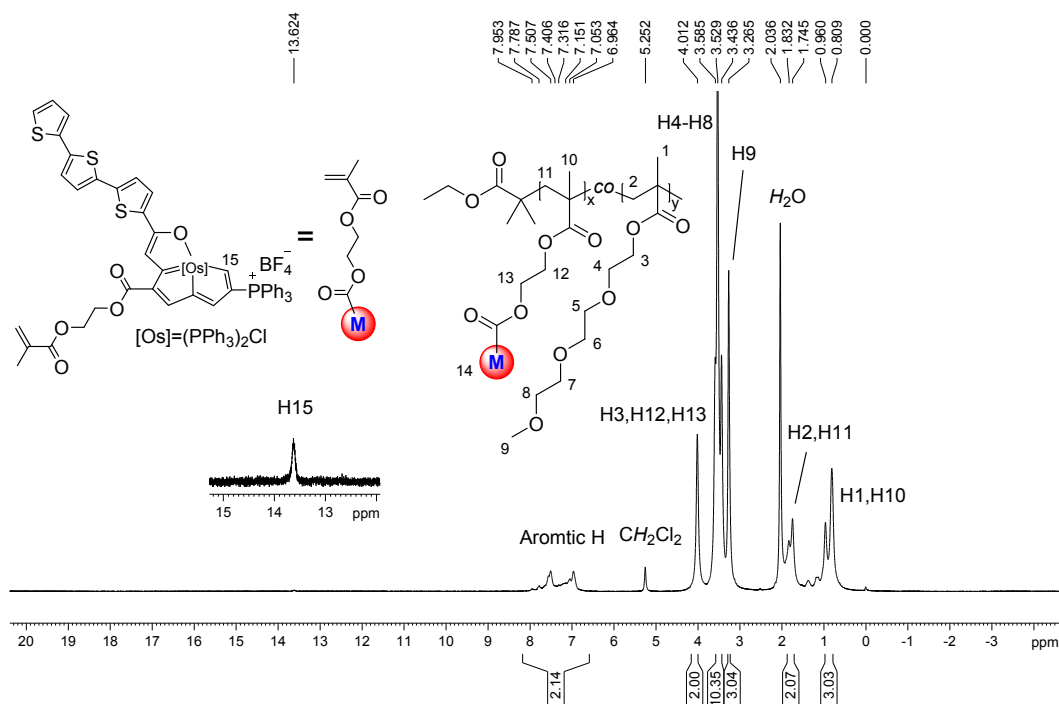


Figure S17 The ^1H NMR (500.2 MHz, CD_2Cl_2) spectrum for copolymer **13**

The unit ratio of **12/14** (x/y) in metallopolymer **13** can be calculated to be 1:26.0 via the integration intensity ratio of aromatic protons (55 aromatic protons per metallopolymer **13**) verse H_9 .

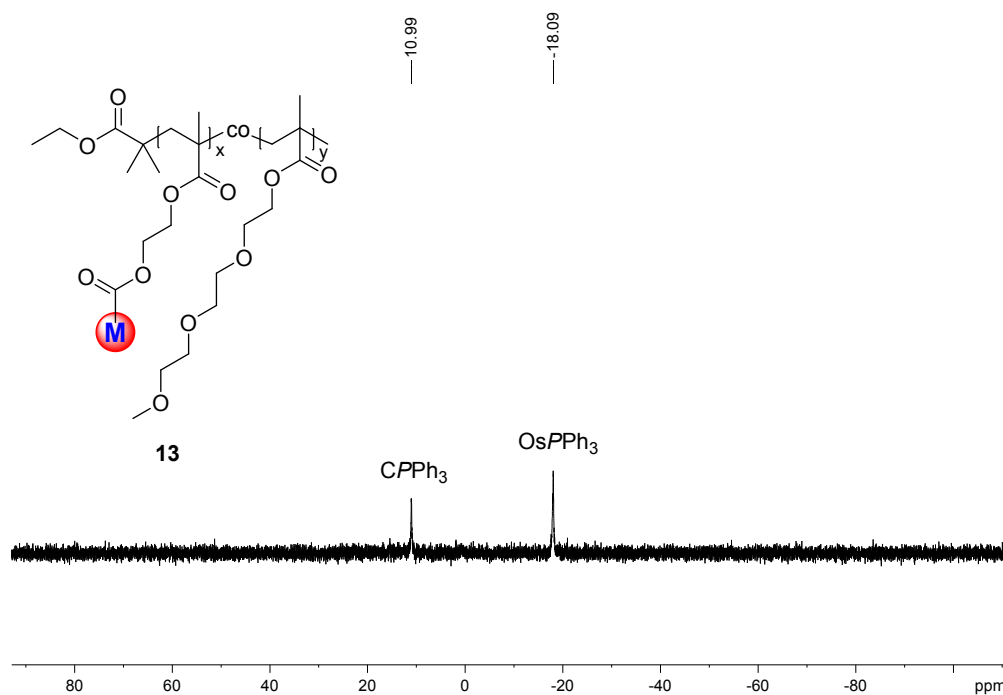


Figure S18 The $^{31}\text{P}\{^1\text{H}\}$ NMR (202.5 MHz, CD_2Cl_2) spectrum for copolymer **13**

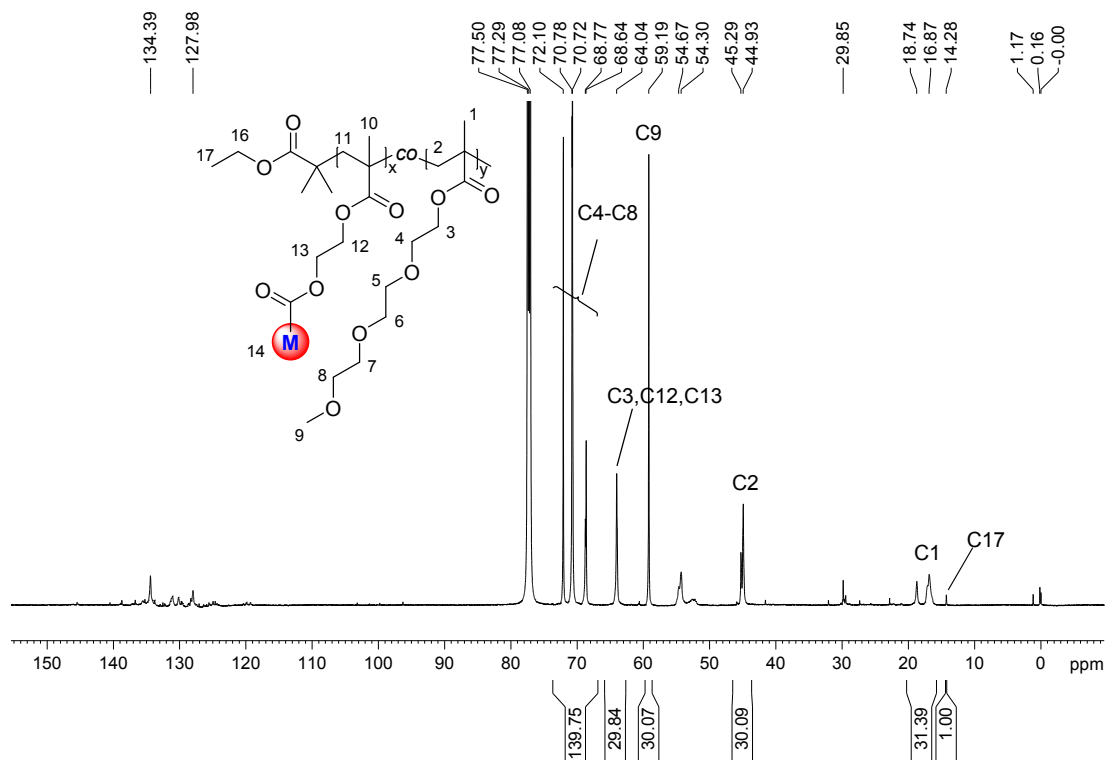


Figure S19 The inverse gated $^{13}\text{C}\{^1\text{H}\}$ NMR (150.9 MHz, CDCl_3) spectrum of copolymer **13**

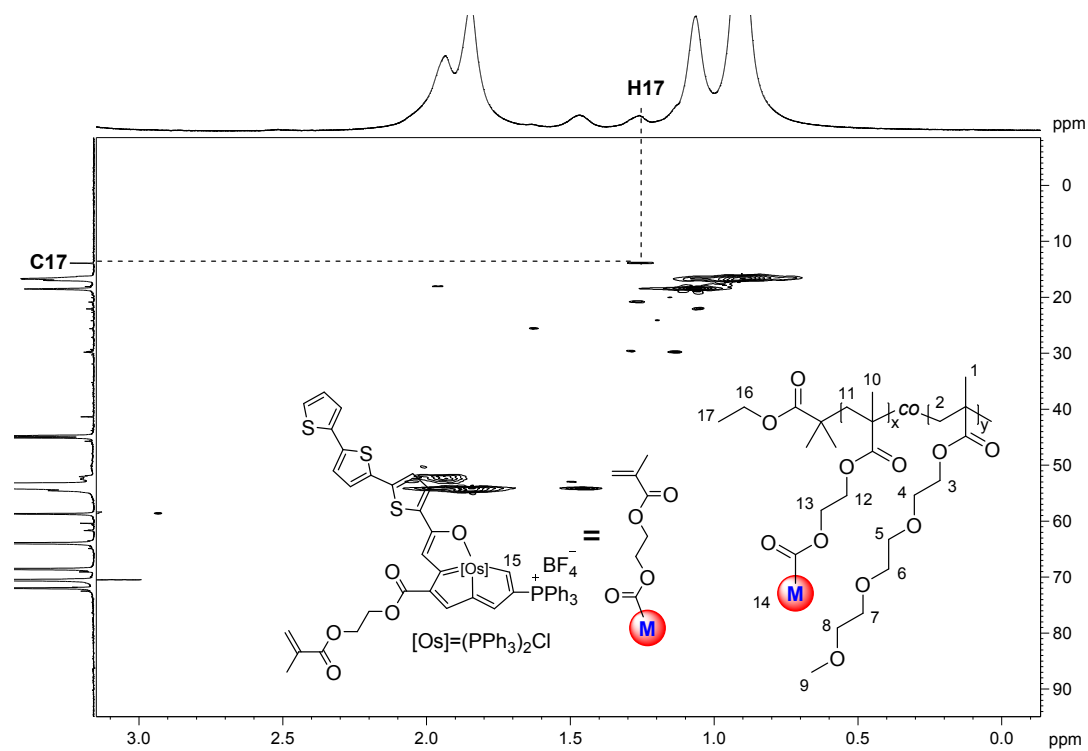


Figure S20 The ^1H - ^{13}C HSQC spectrum of copolymer **13** in CDCl_3 .

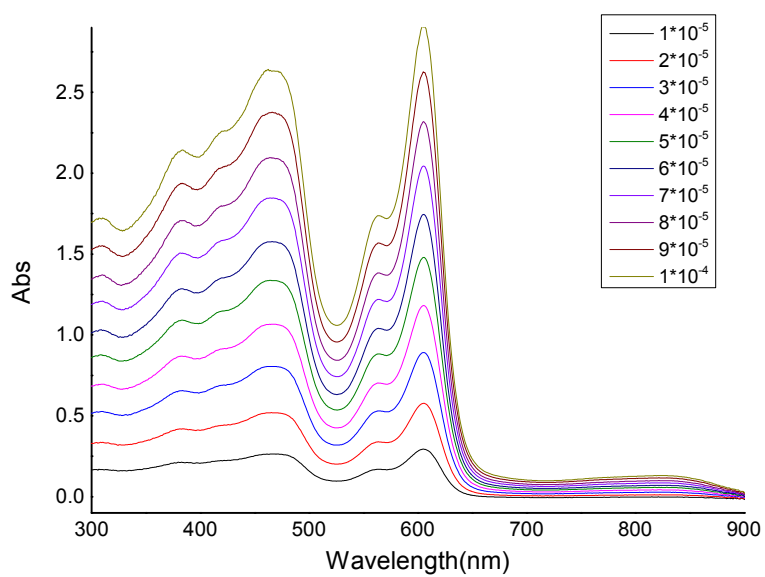


Figure S21 UV-Vis-NIR absorption spectrum of different concentrations of **10** in CH_2Cl_2 .

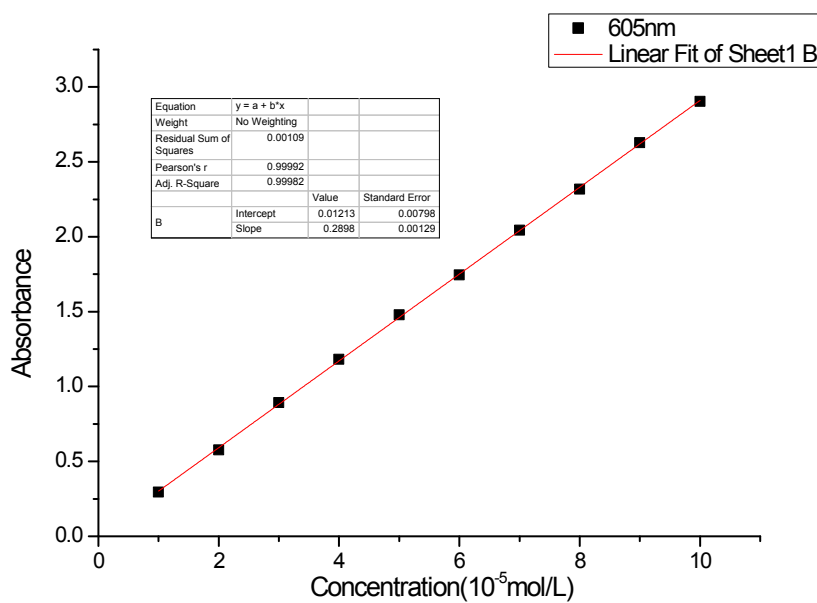


Figure S22 The linear relationship between the concentrations and absorption intensities of **10** at 605 nm.

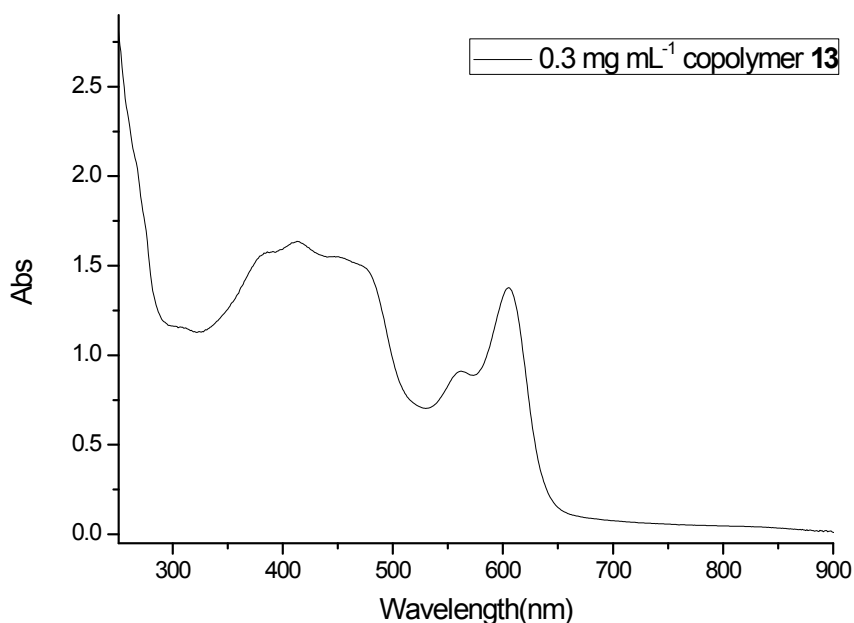


Figure S23 UV-Vis-NIR Absorption spectrum of 0.3 mg/mL **13** in CH₂Cl₂.

The unit ratio of **12/14** (x/y) in metallopolymer **13** was calculated by the following equation:

$$x/y = n_{12}/n_{14} = n_{12}/(W_{14}/M_{14}) = n_{12}/[(W_{\text{all}}-W_{12})/M_{14}] = n_{12}/[(W_{\text{all}}-n_{12}\times M_{12})/M_{14}] = 4.547\times 10^{-5}/[(0.3-4.547\times 10^{-5}\times 1632)/232.3] = 1/21.4$$

Where n_{12} and n_{14} are the molar concentrations of **12** and **14**; n_{12} is calculated to be 4.547×10^{-5} mol/L by using the absorption value in Figure S23 and the standard UV-Vis absorption curve of complex **10** (Figure S22). W_{14} , W_{12} and W_{all} are mass concentrations of **12**, **14** and copolymer **13**, respectively; M_{12} and M_{14} are molecular weights of **12** and **14**.

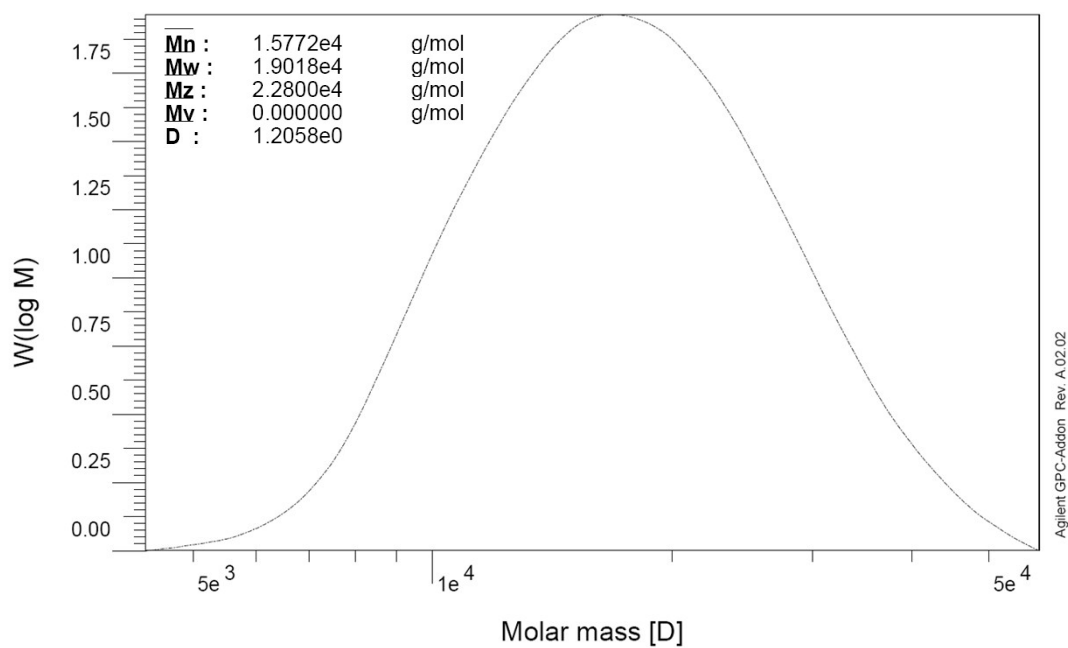


Figure S24 Molecular weight and its distribution of copolymer **13** determined by SEC in tetrahydrofuran relative to narrow molecular weight polystyrenes.

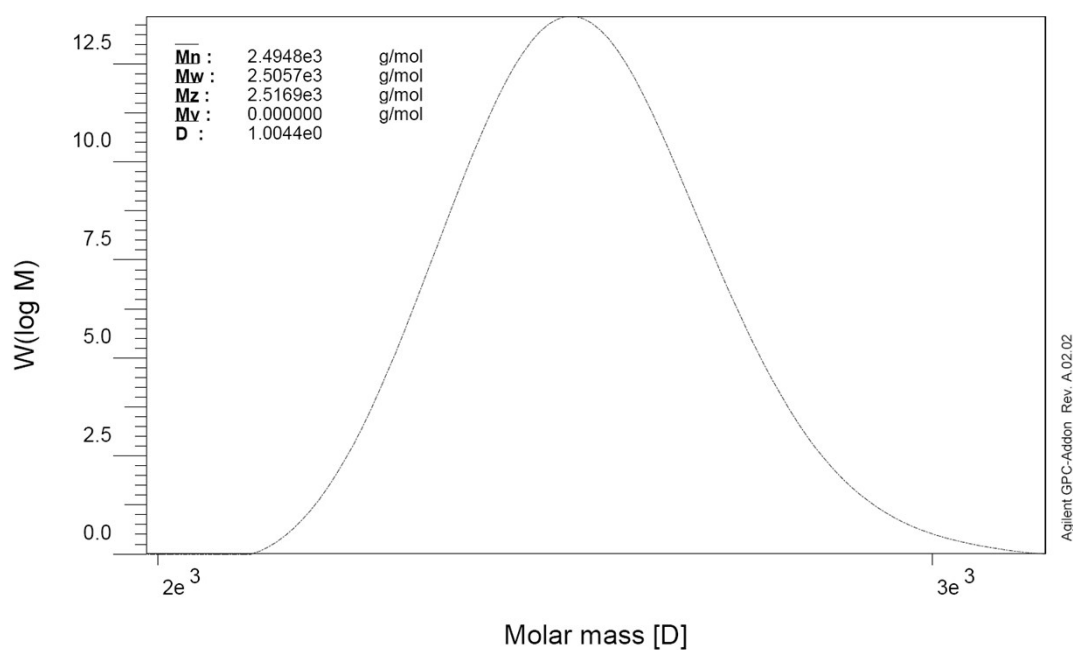


Figure S25 Molecular weight and its distribution of monomer **12** determined by SEC in tetrahydrofuran relative to narrow molecular weight polystyrenes.

2. X-ray molecular structure for 9

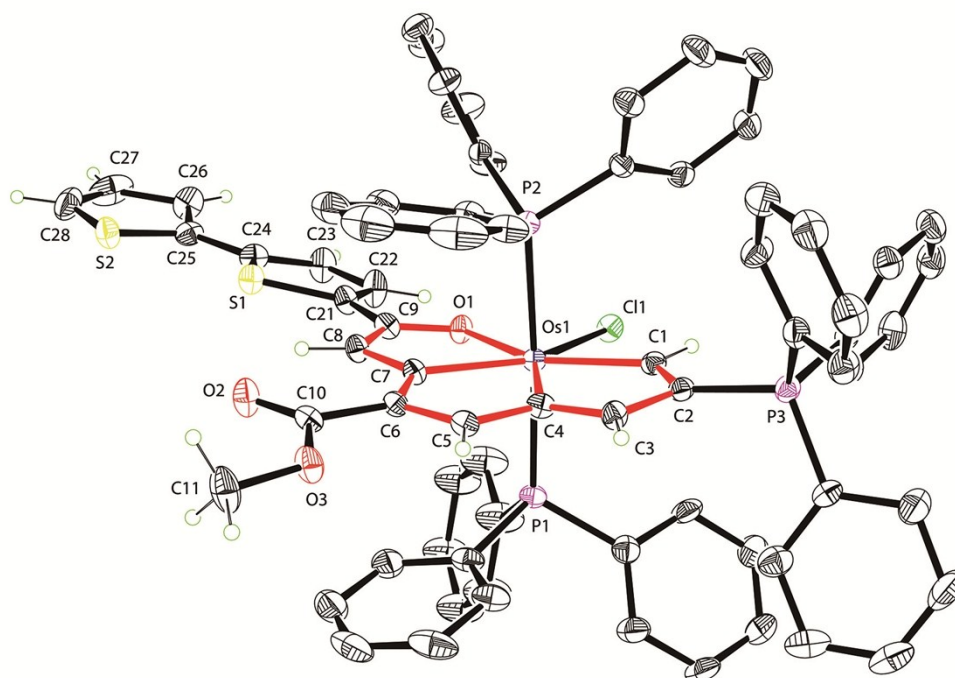


Figure S26 X-ray molecular structure for the cation of **9** (ellipsoids set at 50% probability). Hydrogen atoms in the PPh₃ groups are omitted for clarity. Selected bond lengths [Å] and angles [°]: Os1–C1 2.091(5), Os1–C4 2.138(5), Os1–C7 2.129(5), Os1–O1 2.108(3), C1–C2 1.348(7), C2–C3 1.426(7), C3–C4 1.350(7), C4–C5 1.420(7), C5–C6 1.349(7), C6–C7 1.440(7), C7–C8 1.376(7), C8–C9 1.377(7), C9–O1 1.298(6); Os1–C1–C2 124.4(4), C1–C2–C3 111.4(5), C2–C3–C4 112.1(5), C3–C4–Os1 122.1(4), C4–Os1–C1 69.99(19), Os1–C4–C5 118.4(4), C4–C5–C6 116.3(5), C5–C6–C7 112.5(4), C6–C7–Os1 120.0(4), C7–Os1–C4 72.7(2), Os1–C7–C8 117.2(4), C7–C8–C9 113.7(5), C8–C9–O1 116.4(5), C9–O1–Os1 119.7(3), O1–Os1–C7 72.67(17).